Gene expression profiles following active HE4 stimulation in epithelial ovarian cancer cells: microarray study and comprehensive bioinformatics analysis

Liancheng Zhu
Shengjing Hospital of China Medical University https://orcid.org/0000-0002-0814-5816
Mingzi Tan
Department of Gynecology, Cancer Hospital of China Medical University, Liaoning Cancer Hospital & Institute, Shenyang 110042, Liaoning, China
Haoya Xu
Department of Obstetrics and Gynecology, Shengjing Hospital of China Medical University, Shenyang, Liaoning 110004, China. Key Laboratory of Maternal-Fetal Medicine of Liaoning Province, Key Laboratory of Obstetrics and Gynecology of Higher Education of Li
Bei Lin (linbei88@hotmail.com)
Department of Obstetrics and Gynecology, Shengjing Hospital of China Medical University, Shenyang, Liaoning 110004, China. Key Laboratory of Maternal-Fetal Medicine of Liaoning Province, Key Laboratory of Obstetrics and Gynecology of Higher Education of Li

Research

Keywords: Human epididymis protein 4, epithelial ovarian cancer, differentially expressed gene, bioinformatics

Posted Date: November 4th, 2020

DOI: https://doi.org/10.21203/rs.3.rs-100248/v1

Abstract

Background: Human epididymis protein 4 (HE4) is a novel serum biomarker for diagnosing epithelial ovarian cancer (EOC) with high specificity and sensitivity, compared with CA125. Recent studies have focused on the roles of HE4 in promoting carcinogenesis and chemoresistance in EOC; however, the molecular mechanisms underlying its action remain poorly understood. This study was conducted to determine the molecular mechanisms underlying HE4 stimulation and identifying key genes and pathways mediating carcinogenesis in EOC by microarray and bioinformatics analysis.

Methods: We established a stable HE4-silenced ES-2 ovarian cancer cell line labeled as “S”; the S cells were stimulated with the active HE4 protein, yielding cells labeled as “S4”. Human whole-genome microarray analysis was used to identify differentially expressed genes (DEGs) in S4 and S cells. The “clusterProfiler” package in R, DAVID, Metascape, and Gene Set Enrichment Analysis were used to perform gene ontology (GO) and pathway enrichment analysis, and cBioPortal was used for WFDC2 coexpression analysis. The GEO dataset (GSE51088) and quantitative real-time polymerase chain reaction were used to validate the results. Protein–protein interaction (PPI) network and modular analyses were performed using Metascape and Cytoscape, respectively.

Results: In total, 713 DEGs were identified (164 upregulated and 549 downregulated) and further analyzed by GO, pathway enrichment, and PPI analyses. We found that the MAPK pathway accounted for a significant large number of the enriched terms. WFDC2 coexpression analysis revealed ten WFDC2-coexpressed genes (*TMEM220A*, *SEC23A*, *FRMD6*, *PMP22*, *APBB2*, *DNAJB4*, *ERLIN1*, *ZEB1*, *RAB6B*, and *PLEKHF1*) whose expression levels were dramatically altered in S4 cells; this was validated using the GSE51088 dataset. Kaplan–Meier survival statistics revealed that all 10 target genes were clinically significant. Finally, in the PPI network, 16 hub genes and 8 molecular complex detections (MCODEs) were identified; the seeds of the five most significant MCODEs were subjected to GO and KEGG enrichment analyses and their clinical relevance was evaluated.

Conclusions: Through microarray and bioinformatics analyses, we identified DEGs and determined a comprehensive gene network following active HE4 stimulation in EOC cells. We proposed several possible mechanisms underlying the action of HE4 and identified the therapeutic and prognostic targets of HE4 in EOC.

Background

Human epididymis protein 4 (HE4) is a member of the WFDC domain family and is encoded by the WFDC2 gene; it features the characteristic WAP motif consisting of eight disulfide bonds formed by cysteines [1]. It was initially discovered in human distal epididymal epithelial cells by Kirchhoff et al. in 1991 [2]. Under physiological conditions, HE4 is secreted into the blood to act as a protease inhibitor and is involved in the maturation of sperm cells [2]. Several types of cancers are associated with HE4 overexpression in both the serum and tissues, and it is a relatively promising and useful biomarker for diagnosing ovarian cancer [3–5], primary fallopian tube carcinoma [6], endometrial cancer (combined with CA125) [7], lung cancer [8], breast cancer (combined with miR-127) [9], gastric cancer [1], colorectal cancer [10], and pancreatic adenocarcinomas [11]. In 2008, HE4 was approved for using as a serum marker to monitor disease recurrence or progression in patients with epithelial ovarian cancer (EOC) by the Food and Drug Administration of USA, and has been examined in many studies. Numerous studies have shown that HE4 is a useful biomarker with higher sensitivity and specificity than CA125 in the early confirmatory diagnosis of EOC and differentiation of pelvic masses, particularly in combination with the risk of ovarian malignancy algorithm [12, 13]; HE4 appears to be a good predictive factor for the choice of tumor cytoreductive surgery [3], pre-operative prediction of residual disease after interval cytoreduction [4], and the prediction of adjuvant chemotherapy resistance [14] and possibility of ascites formation [15].

Most studies on HE4 have focused on its clinical applications, whereas its mechanism or function in EOC has not been widely examined; researchers have not yet reached a consensus with regard to its role in EOC. Previous studies revealed that HE4 overexpression significantly promotes tumor cell apoptosis and adhesion and inhibits cell proliferation, migration, and invasiveness [16, 17]; other researchers showed that high expression of HE4 promotes cell migration, spreading, and proliferation [18]. Further, HE4 may regulate the mitogen-activated protein kinase (MAPK) and phosphoinositide 3-kinase/AKT signal transduction (PI3K/AKT) pathways to exert tumor-suppressive effects *in vitro* [18, 19]. Recently, studies have been carried out to investigate the association between HE4 and tumorigenesis as well as chemotherapeutic resistance in EOC; however, these have shown inconsistent results [20–24].

Gene expression profiling and bioinformatic analysis can be used to retrieve a large amount of biological information accumulated for a specific gene and provide fundamental data for molecular mechanism investigations and to identify new interaction targets. Microarray profiling of active HE4 stimulation within EOC cells has not been performed thus far. Therefore, in this study, we performed microarray analyses to comprehensively analyze the expression profiles in EOC cells following active HE4 stimulation. Differentially expressed genes (DEGs), HE4-coexpressed genes, hub genes, and molecular complex detections (MCODEs) were identified and analyzed by GO, pathway enrichment, and protein-protein interaction (PPI) analyses. The verified coexpressed genes and hub genes may be useful for identifying novel biomarkers and treatment targets in combination with HE4 in ovarian cancer.

Materials And Methods

Cell culture, gene transfection and identification

ES-2 cells were purchased from the American Type Culture Collection (Manassas, VA, USA) and maintained in RPMI-1640 medium containing 10% fetal bovine serum and 1% penicillin/streptomycin at 37°C in a humidified atmosphere with 5% CO_2. Cell culture and construction of short hairpin RNA

(shRNA) expression vectors for HE4 silencing, and gene transfection was performed as previously described [25]. The stable cell line expressing low levels of HE4 and empty plasmid-transfected cell lines were named as “S” and “S_Mock”, respectively. Untreated cells were labeled as “S_Untreated”. Quantitative real-time polymerase chain reaction (qRT-PCR) and western blotting were performed as preciously described [25]to detect the mRNA and protein expresison of HE4 in different groups of cells. Active HE4 protein (recombinant human HE4, rHE4, catalog: MBS355616, MyBioSource) was used to stimulate S cells (serum-free medium containing 0.2 μg/mL recombinant HE4 protein for 24 h) [26]; these were labeled as “S4” cells.

Microarrays and bioinformatics analysis

Microarray analysis was performed using triplicate samples of S cells and S4 cells. Total RNA extraction and quantity control were performed as previously described [25]. RNA purity and integrity pass criteria were established as A260/A280 ≥ 1.8, A260/A230 ≥ 1, and RNA integrity number ≥ 6. Contamination of the samples with genomic DNA was evaluated by agarose gel electrophoresis. Target preparation and hybridization were performed as previously described [25]. The pass criteria for CyDye incorporation efficiency was > 10 dye molecules/1000 nucleotides.

Purified RNA samples were analyzed with the Human Whole Genome OneArray® (Array Version: HOA6.1) containing the Phalanx hybridization buffer using the Phalanx Hybridization System (Phalanx Biotech Group, Hsinchu, Taiwan) for microarray analysis; the hybridization process has been described previously [25]. Fold-change (FC) in gene expression was calculated using Rosetta Resolver 7.2 with the error model adjusted by Amersham Pairwise Ration Builder to compare the signals of different samples. DEGs were identified by volcano plot filtering using the following thresholds: $\log_2|FC| \geq 1$ and p value < 0.05, or log2 ratios is “NA” and differences in intensity between two samples of ≥ 1,000. Hierarchical clustering was performed using the “pheatmap” package in R with the threshold of $\log_2|FC|$ defined as ≥ 2. Gene Ontology (GO) analysis and pathway enrichment were performed using multiple databases, including “clusterProfiler” package in R, DAVID (https://david.ncifcrf.gov), and Metascape [27] (https://metascape.org), using p values < 0.05 as the cut-off threshold. Gene Set Enrichment Analysis (GSEA, Version 4.0.3) was performed according to the software instructions for the comprehensive microarray datasets showing differentially expression of genes to determine differences and enriched gene sets in S4 cells versus those in S cells [28, 29]. In this study, we focused on GO biological processes and pathway processes using the gene sets “c5.bp.v7.1.symbols.gmt”, “c2.cp.biocarta.v7.1.symbols.gmt”, “c2.cp.pid.v7.1.symbols.gmt”, and “c2.cp.reactome.v7.1.symbols.gmt”, which were downloaded from the Molecular Signatures Database (http://www.broadinstitute.org/gsea/). Enrichment analysis was performed using 1000 phenotype permutations and gene sets with a nominal P-value < 0.05, and selecting the weighted scoring scheme with a signal to statistical noise metric to rank genes and perform GSEA [31].

HE4 (WFDC2) coexpression analysis and validation by bioinformatics

Genes coexpressed with *WFDC2* were analyzed using the cBioPortal database (http://www. cbioportal.org). The RNA-Seq V2 RSEM data were obtained from The Cancer Genome Atlas (TCGA) Pancancer Atlas, which includes 585 ovarian serous cystadenocarcinoma tissues. Spearman’s correlation score (≥ 0.2 was considered as positively correlated and ≤ − 0.2 was considered as negatively correlated with *WFDC2*) were used to select *WFDC2*-coexpressed genes. To predict the target genes that were changed according to the microarray analysis, we used the Venny online tool (https://bioinfogp.cnb.csic.es/tools/venny/) to identify overlapping genes among the DEGs and *WFDC2*-coexpressed genes.

To validate the target genes, the gene expression profile result GSE51088, submitted by Slamon et al. [30] was used. This gene expression profile contains 152 tissue samples from patients with EOC, 5 tissue samples from patients with benign epithelial ovarian tumors, and 15 normal healthy ovarian tissue samples. Based on these data, we calculated the Pearson correlation coefficient between the target genes and *WFDC2* and compared the expression of target genes among malignant, benign, and normal ovarian tissues (*t* test, p < 0.05 as the cut-off criterion) with the “ggplot2” and “ggpubr” packages in R. The clinical significance of the target genes was evaluated by Kaplan-Meier survival analysis (http://www.kmplot.com/). A total of 1436 mRNA data samples for progression-free survival (PFS) and 1657 mRNA data samples for overall survival (OS) of EOC was evaluated. The patients were split into 2 groups (high vs. low) based on the expression level of the targets genes.

Validation of target genes by qRT-PCR

To validate the target genes, qRT-PCR was conducted as previously described [25]. Ten target genes were selected and primers for these genes were designed and obtained as previously described. The primer sequences are presented in Table 1. All reactions were performed in triplicate, and the specificity of PCR amplification was determined by melting point curve analysis.

Table 1
Primers for 10 target genes in qRT-PCR validation

Gene name	Sense primer	Anti-sense primer	Product size(bp)
TMEM200A	ATTGGCAGCAAATACGAT	AAGCACTGATGGACGATG	251
SEC23A	AACACTGGTGCTCGTATC	TTGTAGCAGCTCGATTAG	181
FRMD6	GGACACTCTGGGTTGATT	GTCTTTGGTTTCCGACAT	125
PMP22	CCTCAGGAAATGTCCACCAC	CGCACAGACCAGCAAGAA	192
DNAJB4	TTTGGAAGACGAATGGGTG	TCTTGTTTGAGGCGGGAT	137
APBB2	CGAGCCTAATGCTGGTAA	CAAAGTGTCAATGAGGGATA	184
ERLIN1	ACCGAATAGAAGTGGTTAA	GCACAGCCTGTATAGTGA	246
ZEB1	AAGTGGCGGTAGATGGTA	TGTTGTATGGGTGAAGCA	103
RAB6B	CGGTGGCTGTGGTGGTGTA	CCAGGTCCGTCTTGTTGC	132
PLEKHF1	CAAGTGCGGCTTCGTGGTC	CCTCGTCGGAGTCATCGTCA	227

PPI network construction and identification of key modules

Metascape was used to establish a PPI network, and proteins with a degree > 1 were selected. The network analyzer "CentiScape" of Cytoscape software was used to analyze the topology properties of the network. Genes with a degree of connectivity ≥ 30 were defined as hub genes. "Molecular Complex Detection" (MCODE) in Metascape was used to analyze the modules of the PPI network, with the degree cut-off set to 2. The seeds of key modules were identified; then, GO analysis and KEGG pathway analysis were performed and the clinical significance of these modules was evaluated.

Statistical analyses

Statistical analyses were performed using SPSS version 24 software for Mac (SPSS, Inc., Chicago, IL, USA) and GraphPad Prism 8 version 8.21 software for Mac (GraphPad, Inc. San Diego, CA, USA). Quantitative data are presented as the mean ± SD. The *t* test was used to compare the data from two groups. The "ggplot2", "ggpubr", "ggscatterstats", "limma", "pheatmap", "clusterProfiler", and "enrichplot" packages in the R language tool were used (R, Version 3.6.1; RStudio, Version 1.2.5019). P-values < 0.05 were considered as statistically significant.

Results

Identification of HE4 gene transfection and RNA quantity assessment

As detected by qRT-PCR and western blotting, the gene and protein expression levels of HE4 were significantly lower in HE4 shRNA-transfected cells than in the untreated and mock cells (Fig. 1A and B, all P < 0.01), with the latter two groups showing no significant difference in HE4 expression (P > 0.05). Assessment of RNA quantity and purity showed that both samples of S and S4 passed the criteria for amplification yield and labeling efficiency (Table 2).

Table 2
The cell line samples description and RNA qualification

Sample	OD260/280	OD260/230	RIN	Results
S	2.02	2.24	10.0	Pass
S4	2.03	2.08	9.4	Pass

Gene expression analysis and clustering

After hybridizing the chip and obtaining the data, volcano analysis revealed the distribution of the 18,398 expressed genes (Fig. 1C). Setting the $\log_2|FC| \geq 1$ and $P < 0.05$ as the cut-off criteria, 713 DEGs were identified, among which 549 genes were downregulated and 164 genes were upregulated (Fig. 1D, the raw data are shown in Supplementary Table 1, all DEGs are listed in Supplementary Table 2). For DEGs showing differential expression based on $\log_2|FC|$ values ≥ 2, heatmap analysis revealed that 5 DEGs, *EPS15*, *MSMO1*, *TMPO*, *ECT2*, and *ZMYND11*, had higher expression levels in S4 cells than in S cells; 21 DEGs, including *PABPC1*, *AP3S1*, *TMX2*, *PHF6*, *NR1D2*, *RAB23*, and *NEK7*, among others, showed lower expression levels in S4 cells than in S cells (Fig. 1F).

Gene Ontology function analysis of DEGs

We performed Gene Ontology (GO) enrichment analysis by uploading all DEGs to the "clusterProfiler" package in R to determine their biological functions. The DEGs were classified into three functional groups: biological process (BP), cellular component (CC), and molecular function (MF). The most enriched BP functions were coenzyme metabolic process and cofactor biosynthetic process. Nuclear speck and nuclear inner membrane were the most enriched CC terms. In the clusters of MF, single-stranded RNA binding and translation factor activity were the most enriched (Fig. 2A). To gain

additional biological insights, we used Metascape [27] to identify BPs in which the DEGs participated. The results of enrichment analysis related to the significant GO terms selected for the DEGs are shown as a heatmap (Fig. 2B, C). Among the diverse pathways highlighted, various pathways are related to oncogenetics, such as: “cell division”, “DNA repair”, “regulation of growth”, “regulation of DNA metabolic process”, “regulation of mitotic cell cycle”, “phosphatidylinositol phosphorylation”, and “signal transduction by p53 class mediator”, etc. These results confirmed that HE4 participates in the tumorigenesis and development of epithelial ovarian carcinoma cells. Interestingly, the “response to wounding” and “cellular response to glucose starvation” pathway, which were found to be modulated by HE4, were associated with immune response regulation and autophagy, indicating that HE4 may drive immune mediator production and autophagy regulation. For GSEA analysis using the GO biological process as the gene set, 132 items were enriched with nominal P-values < 0.05. The “GO_MAP_KINASE_KINASE_KINASE_ACTIVITY” showed the most significant enrichment, with the highest normalized enrichment score (2.166, nominal P-value = 0) (Supplementary Table 3), indicating that MAPK participates in the tumorigenesis induced by HE4 activation (Fig. 2D).

Pathway enrichment analysis of DEGs

KEGG pathway enrichment analysis of the 713 DEGs was conducted using Metascape [27]. Nineteen KEGG pathways were enriched among the DEGs with the following criteria: minimal overlap ≥ 3, P-value cutoff < 0.01, and minimal enrichment = 1.5. The MAPK signaling pathway, TNF signaling pathway, PI3K-AKT signaling pathway, p53 signaling pathway, and cell cycle were highly enriched in the DEGs, in which the MAPK signaling pathway was the most significantly enriched (Fig. 2E (1)). To analyze and integrate the pathways involved in different gene lists, we divided the DEGs into the up- and downregulated groups and performed pathway analysis using Metascape. Pathway enrichment analysis included pathways currently covered by Metascape: KEGG, Hallmark Gene Sets, Reactome Gene Sets, Canonical, and BioCarta Gene Sets, using the criteria described above. Finally, we found that the MAPK pathway, cell cycle, and PI3K/AKT/mTOR pathways were highly enriched, with the MAPK signaling pathway showing the most significant enrichment in S4 cells, compared to the case in S cells (Fig. 2E (2)). To further explore the expression of the MAPK signaling pathway in different gene datasets within the comprehensive microarray datasets, we performed GSEA. The results showed that the MAPK signaling pathway was significantly enriched in the BioCarta, PID, and Reactome Gene Sets in S4 cells, compared to the case in S cells (all nominal P-value < 0.05, Fig. 2F). These results suggest that the MAPK pathway is critical in the oncogenesis of HE4 in EOC.

HE4 coexpression analysis and validation

Genes coexpressed with HE4 (encoded by *WFDC2*) within EOC cells were identified using cBioPortal, which is based on the TCGA Pancancer atlas and includes 585 ovarian serous cystadenocarcinoma tissues. In total, 870 *WFDC2*-coexpressed genes showed a |Spearman’s correlation score |≥ 0.2 and P-value < 0.05 (Supplementary Table 4). In total, 26 genes overlapped between the DEGs and *WFDC2*-coexpressed genes, including 19 and 7 genes whose expression levels were positively and negatively correlated with HE4, respectively (Table 3). To validate these target genes, the GEO dataset GSE51088 [30], which included 152 patients with EOC (including 11 epithelial ovarian borderline tumors), 5 patients with normal ovarian tumor, and 15 normal healthy ovarian tissues, was used to calculate the correlation coefficient. Ten genes were dramatically correlated with HE4 expression, including 8 that were negatively correlated (*TMEM220A*, *SEC23A*, *FRMD6*, *PMP22*, *APBB2*, *DNAJB4*, *ERLIN1*, and *ZEB1*), and 2 that were positively correlated (*RAB6B* and *PLEKHF1*) with HE4 expression (Fig. 3A). To further validate the microarray data, the ten target genes were subjected to qRT-PCR to detect their differential expression in S and S4 cells (Fig. 3B). The qRT-PCR data were consistent with the gene chip results (all P < 0.05).

Table 3
The genes overlapped between DEGs and WFDC2 coexpressed genes generated from cBioPortal.

	DEGs		cBioPortal		
Genesymbol	LogFC	P.value	Spearman's Correlation	p-Value	q-Value
ETV1	-1.74112926	9.21829E-11	-0.25137639	6.07672E-06	0.000513469
TMEM200A	-1.67330712	9.37E-18	-0.23841013	1.84227E-05	0.001075433
SEC23A	-1.66999494	2.15E-24	-0.21612883	0.000107666	0.003532546
MATR3	-1.65897541	1.52E-37	-0.23665619	2.1305E-05	0.001187558
FBXW7	-1.57957489	6.79E-22	-0.2267981	4.72523E-05	0.002057419
EMC2	-1.49126921	6.49E-15	-0.22135379	7.22909E-05	0.002792783
FRMD6	-1.39540806	1.27E-20	-0.24639449	9.37318E-06	0.000667118
GTF2H3	-1.36037738	3.36E-14	-0.20451604	0.000252306	0.006047828
PMP22	-1.34490578	1.40243E-11	-0.20348488	0.00027152	0.006304242
IREB2	-1.29329478	1.96E-18	-0.25242374	5.54111E-06	0.000488278
TM4SF18	-1.26331644	0.001843692	-0.20174481	0.000307069	0.006797924
BLOC1S6	-1.2311467	2.83E-13	-0.23064443	3.4772E-05	0.001653979
APBB2	-1.21372596	3.68573E-05	-0.25358365	5.00049E-06	0.000462079
ZFAND6	-1.20997926	1.34621E-05	-0.20588664	0.000228727	0.005643468
DNAJB4	-1.18965026	4.7754E-11	-0.22039349	7.78373E-05	0.002944791
RANBP2	-1.16466642	1.6059E-09	-0.2361569	2.22005E-05	0.001214792
ERLIN1	-1.14961785	8.98E-17	-0.20737172	0.000205512	0.005308028
SLK	-1.08761539	3.19422E-09	-0.23495397	2.45069E-05	0.001288354
ZEB1	-1.01529781	1.18109E-09	-0.24887479	7.56265E-06	0.000576294
MKNK2	1.03904918	2.28E-16	0.22219649	6.77323E-05	0.00265548
SMARCD3	1.04293745	4.82E-16	0.26206354	2.32529E-06	0.00027583
RAB6B	1.06900496	2.2E-14	0.20381363	0.000265251	0.006227877
NOXA1	1.07467178	7.95927E-06	0.2024282	0.000292619	0.006587495
IQSEC2	1.10423888	9.16904E-08	0.24086495	1.50035E-05	0.000929112
PLEKHF1	1.11966989	0.001304667	0.38517331	1.29E-12	2.98E-09
RAPGEF3	1.30138476	3.89773E-11	0.24899116	7.48646E-06	0.000574842

To evaluate the clinical significance of these 10 target genes, we determined the correlation between the tumor type and these ten genes in GESE51088, which showed that all ten genes were significantly correlated with tumor types. *TMEM220A*, *SEC23A*, *FRMD6*, *PMP22*, *APBB2*, *DNAJB4*, *ERLIN1*, and *ZEB1* were markedly downregulated in ovarian cancers, compared to the case in ovarian benign tumors and normal tissues, and *RAB6B* and *PLEKHF1* were markedly upregulated in ovarian cancers, compared to the case in ovarian benign tumors and normal tissues (Fig. 4A). Kaplan-Meier survival analysis was performed for a large cohort of patients with ovarian cancer. Data from 1657 patients with EOC were evaluated and the hazard ratios and p-values were determined, as shown in Table 4. Interestingly, all 10 target genes were correlated with overall prognosis (Fig. 4B). These 10 target genes should be further investigated to explore their association with HE4 expression, which may reveal the mechanisms underlying the role of HE4 in EOC development.

Table 4
Validation of 10 WFDC2 co-expressed genes among DEGs

Gene symbol	Microarray analysis		cBioPortal (585 Epithelial ovarian tissues)		GSE51088		Survival Curve (1657 EOC tissues)	
	LogFC	-log10(P.value)	Spearman's Correlation	-log10(P.value)	Pearson score R	-log10(P.value)	HR	LogRank p-value
TMEM200A	-1.6733071	17.0282604	-0.2384101	4.73463965	-0.5306474	13.1530447	1.50 (1.20–1.88)	3e-04
SEC23A	-1.6699949	23.6675615	-0.2161288	3.96790529	-0.3638438	6.03198429	1.25 (1.09–1.42)	0.0011
FRMD6	-1.3954081	19.8961963	-0.2463945	5.02811212	-0.2713641	3.49854362	1.59 (1.29–1.95)	7.5e-06
PMP22	-1.3449058	10.8531188	-0.2034849	3.56619818	-0.4983522	11.4571746	1.45 (1.27–1.65)	3e-08
APBB2	-1.213726	4.43347648	-0.2535836	5.30098657	-0.2996121	4.18508682	1.27 (1.09–1.48)	0.0022
DNAJB4	-1.1896503	10.3209902	-0.2203935	4.10881391	-0.4288876	8.36066295	1.31 (1.14–1.51)	0.00017
ERLIN1	-1.1496178	16.0467237	-0.2073717	3.68716704	-0.2856046	3.83564714	0.87 (0.76–0.99)	0.034
ZEB1	-1.0152978	8.92771701	-0.2488748	5.12132313	-0.4347875	8.59749789	1.60 (1.28–1.99)	2.2e-05
RAB6B	1.06900496	13.6575773	0.20381363	3.57634461	0.2067661	2.18706059	1.34 (1.05-.170)	0.017
PLEKHF1	1.11966989	2.88450032	0.38517331	11.8894103	0.2926423	4.00899113	1.17 (1.02–1.35)	0.03

PPI network and modular analysis

PPI enrichment analysis was carried out in Metascape. The resultant network contained the subset of proteins that physically interact with at least one other member in the gene list. The “centiscape” plug-in in Cytoscape was used to identify the hub genes, and proteins with degree > 1 were selected. In total, 289 nodes (40.4% of all 713 DEGs) and 2942 PPI relationships were obtained (Fig. 5A). Sixteen genes with a degree of connectivity > 30 were defined as hub genes for HE4 activation (Table 5). According to the degree rank, the 16 hub genes were *HSPA1B*, *HSPA1A*, *SUMO1*, *CDK1*, *MAX*, *PABPC1*, *MAGOH*, *HNRNPU*, *YWHAG*, *RANBP2*, *SRSF1*, *CNBP*, *U2AF2*, *RNPS1*, *SMAD3*, and *POLR2D*. These hub genes interact with each other, suggesting that they play important roles in HE4 activation and should be further studied in EOC.

Table 5
16 hub genes (degree ≥ 30) selected from PPI network according to the degree

Gene Symbol	Eccentricity	Closeness	Betweenness	Degree	Stress
HSPA1B	0.25	0.00198413	12720.52992	93	91258
HSPA1A	0.25	0.00193798	9887.649848	87	77174
SUMO1	0.25	0.00182482	12090.55822	74	77170
CDK1	0.25	0.00166945	7451.126297	59	44320
MAX	0.2	0.00168634	11030.17839	57	61586
PABPC1	0.25	0.00167224	3561.121821	46	26550
MAGOH	0.25	0.00162602	1812.074639	39	16986
HNRNPU	0.25	0.00162866	2527.645484	37	17974
YWHAG	0.25	0.0016129	2749.807044	36	20970
RANBP2	0.25	0.00158479	2066.126067	35	18706
SRSF1	0.25	0.00141844	1366.01731	35	10966
CNBP	0.25	0.0015748	1558.185614	34	14340
U2AF2	0.2	0.00144718	901.9806448	33	7256
RNPS1	0.25	0.00152207	514.6918118	31	6640
SMAD3	0.2	0.00160514	3586.354138	31	23532
POLR2D	0.25	0.0015674	760.9759902	30	8880

The MCODE algorithm [31] was implemented in Metascape to distinguish densely connected network components; 8 modules were identified and sequenced, showing descending scores from 8.65 to 1.00 (Supplementary Table 5). The five most significant MCODEs were extracted when the cut-off score was > 2 (Fig. 5B).

To further explore the biological function of the seeds in the five key modules (*SMNDC1*, *HSPA1A*, *FNBP1L*, *GAR1*, and *SKA2*), functional enrichment analysis was performed based on Metascape by setting the minimum overlap = 2 and P value cutoff = 0.05. The main enriched GO terms were the regulation of microtubule polymerization or depolymerization and positive regulation of cellular component biogenesis. Pathway signaling analysis showed a marked enrichment of the cell cycle and spliceosome (Fig. 5C).

To determine the clinical significance of the 5 seed genes in the key modules, Kaplan-Meier survival analyses were performed for a large ovarian cancer cohort. Data from 1657 and 1436 patients with EOC were evaluated to determine the OS and PFS, respectively, and hazard ratios and p-values were determined. As shown in Fig. 5D, all 5 seed genes were clearly correlated with OS and PFS.

Discussion

Ovarian cancer is the seventh most common malignant tumor worldwide. In 2012, there were an estimated 238,719 cases of ovarian cancer, showing an age-standardized rate of 6.1/100,000 [32]. The American Cancer Society predicted that in 2020, there will be approximately 21,750 new ovarian cancer cases in the United States, and 13,9400 women will die from this disease. Because of its occult onset and innocuous symptoms, most patients with ovarian cancer are diagnosed at an advanced stage. Despite the development of new anti-tumor drugs and improvements in surgical treatment, the survival rates for ovarian cancer decline dramatically from 92% for patients with stage I disease to 17–28% for those with the advanced stages of this disease (stages III–IV) [33]; most patients at an advanced stage eventually relapse and show chemotherapeutic resistance. Although the serum biomarker CA125 is widely used in clinical practice for the diagnosis and differentiation of ovarian cancer, population-based screening of serum CA125 and use of the risk for ovarian cancer algorithm (ROCA) did not result in significant mortality reduction and is thus, ineffective [34]. Thus, the mechanism underlying the oncogenesis of EOC must be determined, and the identification of tumor biomarkers is necessary to facilitate the early diagnosis and targeted therapy or prevention of this disease.

As a new tumor biomarker, HE4 has gained attention in recent years. However, most studies focused on its clinical application with regard to the early and differential diagnosis of EOC, and the prediction of relapse, prognosis, chemotherapeutic resistance, as well as other clinical aspects of EOC [12, 35]; few studies have been performed to determine the mechanism underlying its role in ovarian cancer. This may be because HE4 is not considered as a therapeutic target, as its roles in EOC tumorigenesis and progression remain controversial. In 2011, Gao et al. [16] reported that the overexpression of HE4 markedly promoted ovarian cancer cell apoptosis and adhesion, and that HE4 may inhibit ovarian cancer cell proliferation, migration, and invasiveness, as well as xenograft tumor formation *in vivo*; thus, they concluded that HE4 may play a protective role in the progression of EOC. In 2014, Kong et al. [19] performed *in vitro* studies that showed that this protective influence may be attributed to the regulation of the MAPK and PI3K/AKT pathways. In contrast, other researchers noted that high HE4 expression promotes cell migration, adhesion, proliferation, and spreading, which are associated with

effects on the EGFR-MAPK signaling pathway [18, 36]. Additionally, HE4 contains a fucosylated modification (Lewis y antigen) [37], the overexpression of which can promote HE4-mediated invasion and metastasis in ovarian cancer cells [38]. Overexpression of Lewis y antigen enhanced the tyrosine phosphorylation of EGFR and HER/neu, improving cell proliferation via the PI3K/AKT and Raf/MEK/MAPK pathways [39]. Based on these results, Lewis y antigen and HE4 may affect similar signaling pathways to promote tumor growth and malignancy [40]. HE4 overexpression promotes ovarian cancer cell xenograft tumor growth *in vivo*, which can be suppressed by an antisense target of HE4. HE4 interacts with tumor microenvironment constituents (EGFR, IGF1R, insulin) and the transcription factor HIF1α, supporting that HE4 is related to growth factor signaling and the MAPK/ERK pathway [41]. Annexin A2 was identified as a robust interacting partner of HE4 by mass spectrometry and co-immunoprecipitation, and the HE4-Annexin A2 complex was found to promote the invasion and migration abilities of ovarian cancer cells *in vitro* and tumor distant metastasis of the lung *in vivo*. Downregulation of HE4 decreases the expression of MKNK2 and LAMB2, which are associated with MAPK signaling pathways and focal adhesion [5].

In recent years, an increasing number of studies have shown that HE4 promotes the proliferation, adhesion, invasion, migration, and chemoresistance in ovarian cancer cells [20–26, 42–47]. HE4 overexpression in, or recombinant HE4 treatment of, EOC cells resulted in the upregulation of many transcripts coding for extracellular matrix proteins, including LAMC2, LAMB3, SERPINB2, and GREM1; moreover, in cells overexpressing HE4 or those exposed to recombinant HE4 in the culture medium, the protein levels of LAMC2 and LAMB3 were observed to continuously increase. In the presence of fibronectin, focal adhesions were elevated in cells treated with recombinant HE4 [22].

Ovarian cancer participates in the evasion of immunosurveillance and orchestrates a suppressive immune microenvironment. A series of studies by James et al. [23, 44, 45] showed that upon exposure of purified human peripheral blood mononuclear cells to HE4, osteopontin (OPN) and DUSP6 were the most downregulated and upregulated genes, respectively. The proliferation of human ovarian carcinoma cells in conditioned media from HE4-exposed peripheral blood mononuclear cells was enhanced, whereas this effect was attenuated by adding recombinant OPN or OPN-inducible cytokines (interleukin-12 and interferon-γ). HE4 can compromise both OPN-mediated T cell activation [44] and the activity of cytotoxic $CD8^+/CD56^+$ cells by upregulating self-produced DUSP6 [45], thus promoting the tumorigenesis of ovarian cancer [23, 44, 45, 48]. Other researchers revealed that HE4 promotes the carcinogenesis of ovarian cancer by combining with histone deacetylase 3 to activate the PI3K/AKT pathway [46], and that HE4 knockdown suppresses the invasive cell growth and malignant progress of ovarian cancer by inhibiting the JAK/STAT3 pathway [24]. Few studies have examined the role of HE4 in the chemoresistance of ovarian cancer. Overexpression of HE4 promotes the collateral resistance of ovarian cancer cells to cisplatin and paclitaxel, and downregulation of HE4 partially reverses the resistance of ovarian cancer cells to multiple chemotherapeutic agents; HE4-mediated chemoresistance may be related to various factors, including deregulation of MAPK signaling (EGR1 and p38 inhibition) and alterations of tubulin levels or stability. Recombinant HE4 may upregulate the levels of α-tubulin, β-tubulin, and microtubule-associated protein tau [41, 43]. Similarly, *in vitro*, HE4 represses apoptosis induced by carboplatin, and recombinant HE4 results in increased Bcl-2 expression and decreased Bax (Bcl-2-associated X protein) expression in carboplatin-treated ovarian cancer cells, reducing the Bax/Bcl-2 ratio. In addition, HE4 suppresses EGR1 expression, which may contribute to the overall reduction of the expression of pro-apoptotic factors that lead to EOC chemoresistance [26]. HE4 can enhance the regulation of, and is positively correlated with, DUSP6 expression. DUSP6 deactivates extracellular signal-regulated kinase (ERK), and inhibition of DUSP6 can alter the gene expression of ERK pathway response genes (EGR1 and c-JUN) and sensitize ovarian cancer cells to chemotherapeutic agents (paclitaxel or carboplatin) [23, 48]. Resensitization of ovarian cancer cells to cisplatin and paclitaxel caused by HE4 knockdown occurs because of corresponding decreases in the activities of ERK and AKT pathway-associated genes during gene knockout, and the activation of these pathways inhibits apoptotic signaling in tumor cells [21].

Conclusion

The mechanism underlying the contribution of HE4 to EOC tumorigenesis, progression, and chemoresistance remains unclear. Microarray analysis of HE4 can provide high-throughput data for accurate molecular function research. In this study, we analyzed changes in the gene expression profiles after the stimulation of EOC cells with the active HE4 protein and determined the cellular biological processes involved, to delineate the enriched pathways and interaction networks. We found 713 DEGs (164 upregulated and 549 downregulated genes), with the MAPK pathway accounting for a significant proportion of the enriched terms. *WFDC2* coexpression analysis revealed ten WFDC2-coexpressed genes (*TMEM220A*, *SEC23A*, *FRMD6*, *PMP22*, *APBB2*, *DNAJB4*, *ERLIN1*, *ZEB1*, *RAB6B*, and *PLEKHF1*) whose expression levels were dramatically changed in S4 cells. All 10 target genes were clinically important. Finally, 16 hub genes and 8 MCODEs were identified in the PPI, and the seeds of the five most significant MCODEs were evaluated by enrichment analysis and their clinical significance was determined. Our data provide a foundation for further clarifying the mechanism underlying the role of HE4 in the oncogenesis and chemoresistance of EOC.

Abbreviations

CA125: cancer antigen 125; HE4:human epididymis protein 4; DEG:differentially expressed gene; EOC:epithelial ovarian cancer; GO:gene ontology; GSEA:gene set enrichment analysis; MAPK:mitogen-activated protein kinase; PI3K/AKT:phosphoinositide 3-kinase/AKT signal transduction; PPI:protein-protein interaction; ROCA:risk for ovarian cancer algorithm; shRNA:short hairpin RNA.

Declarations

Ethics approval and consent to participate

Not applicable.

Consent for publication

Not applicable.

Availability of data and materials

The datasets used and/or analyzed during the current study are available from the corresponding author on reasonable request.

Competing interests

We declare that we do not have any commercial or associative interest that represents a conflict of interest in connection with the work submitted.

Funding

The present study was funded by the National Natural Science Foundation of China (grant nos. 81472437 and 81672590), National Natural Science Foundation of China Youth Science Foundation (No. 81602438), Doctoral start-up fund of Liaoning Province (Grant No. 201601133) and 345 Talent Project of Shengjing Hospital.

Authors' contributions

All authors have made substantial contributions to the work including editing and writing assistance reported in the manuscript. LC Z and B L conceived and designed the idea to this paper; LC Z and HY X collected and analyzed the data and drafted the paper; LC Z and MZ T analyzed the data and revised the final paper. The first draft of the manuscript was written by LC Z and all authors commented on previous versions of the manuscript. The whole experimental process was supervised and guided by B L. All authors read and approved the final manuscript.

Acknowledgements

Not applicable.

Authors' information

[1]Department of Obstetrics and Gynecology, Shengjing Hospital of China Medical University, Shenyang, Liaoning 110004, China; [2]Key Laboratory of Maternal-Fetal Medicine of Liaoning Province, Key Laboratory of Obstetrics and Gynecology of Higher Education of Liaoning Province, Liaoning, China; [3]Department of Gynecology, Cancer Hospital of China Medical University, Liaoning Cancer Hospital & Institute, Shenyang 110042, Liaoning, China.

References

1. Peng C, Liu G, Huang K, Zheng Q, Li Y, Yu C. Hypoxia-Induced Upregulation of HE4 Is Responsible for Resistance to Radiation Therapy of Gastric Cancer. Mol Ther Oncolytics. 2019;12:49–55.
2. Kirchhoff C, Habben I, Ivell R, Krull N. A major human epididymis-specific cDNA encodes a protein with sequence homology to extracellular proteinase inhibitors. Biol Reprod. 1991;45(2):350–7.
3. Chen WT, Gao X, Han XD, Zheng H, Guo L, Lu RQ. HE4 as a serum biomarker for ROMA prediction and prognosis of epithelial ovarian cancer. Asian Pac J Cancer Prev. 2014;15(1):101–5.
4. Lof P, van de Vrie R, Korse CM, van Driel WJ, van Gent M, Karlsen MA, Amant F, Lok CAR. Pre-operative prediction of residual disease after interval cytoreduction for epithelial ovarian cancer using HE4. International journal of gynecological cancer: official journal of the International Gynecological Cancer Society. 2019;29(8):1304–10.
5. Zhuang H, Tan M, Liu J, Hu Z, Liu D, Gao J, Zhu L, Lin B. Human epididymis protein 4 in association with Annexin II promotes invasion and metastasis of ovarian cancer cells. Mol Cancer. 2014;13:243.
6. Mi D, Zhang YX, Wang CJ, Feng Q, Qi P, Chen SQ. Diagnostic and prognostic value of serum human epididymis protein 4 in patients with primary fallopian tube carcinoma. J Obstet Gynaecol Res. 2016;42(10):1326–35.
7. Huang GQ, Xi YY, Zhang CJ, Jiang X. Serum Human Epididymis Protein 4 Combined with Carbohydrate Antigen 125 for Endometrial Carcinoma Diagnosis: A Meta-Analysis and Systematic Review. Genet Test Mol Biomarkers. 2019;23(8):580–8.
8. He YP, Li LX, Tang JX, Yi L, Zhao Y, Zhang HW, Wu ZJ, Lei HK, Yu HQ, Nian WQ, et al. HE4 as a biomarker for diagnosis of lung cancer: A meta-analysis. Med (Baltim). 2019;98(39):e17198.
9. Lu M, Ju S, Shen X, Wang X, Jing R, Yang C, Chu H, Cong H. Combined detection of plasma miR-127-3p and HE4 improves the diagnostic efficacy of breast cancer. Cancer Biomark. 2017;18(2):143–8.
10. Shi LP, Guo HL, Su YB, Zheng ZH, Liu JR, Lai SH. MicroRNA-149 sensitizes colorectal cancer to radiotherapy by downregulating human epididymis protein 4. Am J Cancer Res. 2018;8(1):30–8.
11. O'Neal RL, Nam KT, LaFleur BJ, Barlow B, Nozaki K, Lee HJ, Kim WH, Yang HK, Shi C, Maitra A, et al. Human epididymis protein 4 is up-regulated in gastric and pancreatic adenocarcinomas. Hum Pathol. 2013;44(5):734–42.
12. Zhang L, Chen Y, Wang K. Comparison of CA125, HE4, and ROMA index for ovarian cancer diagnosis. Curr Probl Cancer. 2019;43(2):135–44.

13. Brenk A, Bodzek P, Balis M, Barbachowska A, Janosz I, Olejek A. Usefulness of HE4 protein in differentiation of pelvic masses in woman. Prz Menopauzalny. 2019;18(1):27–32.
14. Aarenstrup Karlsen M, Hogdall C, Nedergaard L, Philipsen Prahm K, Schou Karlsen NM, Weng Ekmann-Gade A, Henrichsen Schnack T, Svenstrup Poulsen T, Jarle Christensen I, Hogdall E. HE4 as a predictor of adjuvant chemotherapy resistance and survival in patients with epithelial ovarian cancer. APMIS. 2016;124(12):1038–45.
15. Liu D, Kong D, Li J, Gao L, Wu D, Liu Y, Yang W, Zhang L, Zhu J, Jin X. HE4 level in ascites may assess the ovarian cancer chemotherapeutic effect. J Ovarian Res. 2018;11(1):47.
16. Gao L, Cheng HY, Dong L, Ye X, Liu YN, Chang XH, Cheng YX, Chen J, Ma RQ, Cui H. The role of HE4 in ovarian cancer: inhibiting tumour cell proliferation and metastasis. J Int Med Res. 2011;39(5):1645–60.
17. Dai C, Zheng Y, Li Y, Tian T, Wang M, Xu P, Deng Y, Hao Q, Wu Y, Zhai Z, et al. Prognostic values of HE4 expression in patients with cancer: a meta-analysis. Cancer Manag Res. 2018;10:4491–500.
18. Lu R, Sun X, Xiao R, Zhou L, Gao X, Guo L. Human epididymis protein 4 (HE4) plays a key role in ovarian cancer cell adhesion and motility. Biochem Biophys Res Commun. 2012;419(2):274–80.
19. Kong X, Chang X, Cheng H, Ma R, Ye X, Cui H. Human epididymis protein 4 inhibits proliferation of human ovarian cancer cells via the mitogen-activated protein kinase and phosphoinositide 3-kinase/AKT pathways. International journal of gynecological cancer: official journal of the International Gynecological Cancer Society. 2014;24(3):427–36.
20. Zhu L, Zhuang H, Wang H, Tan M, Schwab CL, Deng L, Gao J, Hao Y, Li X, Gao S, et al. Overexpression of HE4 (human epididymis protein 4) enhances proliferation, invasion and metastasis of ovarian cancer. Oncotarget. 2016;7(1):729–44.
21. Lee S, Choi S, Lee Y, Chung D, Hong S, Park N. Role of human epididymis protein 4 in chemoresistance and prognosis of epithelial ovarian cancer. J Obstet Gynaecol Res. 2017;43(1):220–7.
22. Ribeiro JR, Gaudet HM, Khan M, Schorl C, James NE, Oliver MT, DiSilvestro PA, Moore RG, Yano N. Human Epididymis Protein 4 Promotes Events Associated with Metastatic Ovarian Cancer via Regulation of the Extracelluar Matrix. Front Oncol. 2017;7:332.
23. James NE, Beffa L, Oliver MT, Borgstadt AD, Emerson JB, Chichester CO, Yano N, Freiman RN, DiSilvestro PA, Ribeiro JR. Inhibition of DUSP6 sensitizes ovarian cancer cells to chemotherapeutic agents via regulation of ERK signaling response genes. Oncotarget. 2019;10(36):3315–27.
24. Wang A, Jin C, Tian X, Wang Y, Li H. Knockdown of HE4 suppresses aggressive cell growth and malignant progression of ovarian cancer by inhibiting the JAK/STAT3 pathway. *Biol Open* 2019, 8(9).
25. Zhu L, Guo Q, Jin S, Feng H, Zhuang H, Liu C, Tan M, Liu J, Li X, Lin B. Analysis of the gene expression profile in response to human epididymis protein 4 in epithelial ovarian cancer cells. Oncol Rep. 2016;36(3):1592–604.
26. Wang H, Zhu L, Gao J, Hu Z, Lin B. Promotive role of recombinant HE4 protein in proliferation and carboplatin resistance in ovarian cancer cells. Oncol Rep. 2015;33(1):403–12.
27. Zhou Y, Zhou B, Pache L, Chang M, Khodabakhshi AH, Tanaseichuk O, Benner C, Chanda SK. Metascape provides a biologist-oriented resource for the analysis of systems-level datasets. Nat Commun. 2019;10(1):1523.
28. Mootha VK, Lindgren CM, Eriksson K-F, Subramanian A, Sihag S, Lehar J, Puigserver P, Carlsson E, Ridderstråle M, Laurila E, et al. PGC-1α-responsive genes involved in oxidative phosphorylation are coordinately downregulated in human diabetes. Nat Genet. 2003;34(3):267–73.
29. Subramanian A, Tamayo P, Mootha VK, Mukherjee S, Ebert BL, Gillette MA, Paulovich A, Pomeroy SL, Golub TR, Lander ES, et al: Gene set enrichment analysis: A knowledge-based approach for interpreting genome-wide expression profiles. *Proceedings of the National Academy of Sciences* 2005, 102(43):15545–15550.
30. Karlan BY, Dering J, Walsh C, Orsulic S, Lester J, Anderson LA, Ginther CL, Fejzo M, Slamon D. POSTN/TGFBI-associated stromal signature predicts poor prognosis in serous epithelial ovarian cancer. Gynecol Oncol. 2014;132(2):334–42.
31. Bader GD, Hogue CW. An automated method for finding molecular complexes in large protein interaction networks. BMC Bioinformatics. 2003;4:2.
32. Zhang Y, Luo G, Li M, Guo P, Xiao Y, Ji H, Hao Y. Global patterns and trends in ovarian cancer incidence: age, period and birth cohort analysis. BMC Cancer. 2019;19(1):984.
33. Doubeni CA, Doubeni AR, Myers AE. Diagnosis and Management of Ovarian Cancer. Am Fam Physician. 2016;93(11):937–44.
34. Jacobs IJ, Menon U, Ryan A, Gentry-Maharaj A, Burnell M, Kalsi JK, Amso NN, Apostolidou S, Benjamin E, Cruickshank D, et al. Ovarian cancer screening and mortality in the UK Collaborative Trial of Ovarian Cancer Screening (UKCTOCS): a randomised controlled trial. Lancet. 2016;387(10022):945–56.
35. Dochez V, Randet M, Renaudeau C, Dimet J, Le Thuaut A, Winer N, Thubert T, Vaucel E, Caillon H, Ducarme G. Efficacy of HE4, CA125, Risk of Malignancy Index and Risk of Ovarian Malignancy Index to Detect Ovarian Cancer in Women with Presumed Benign Ovarian Tumours: A Prospective, Multicentre Trial. *J Clin Med* 2019, 8(11).
36. Chen Y, Mu X, Wang S, Zhao L, Wu Y, Li J, Li M. WAP four-disulfide core domain protein 2 mediates the proliferation of human ovarian cancer cells through the regulation of growth- and apoptosis-associated genes. Oncol Rep. 2013;29(1):288–96.
37. Zhuang H, Gao J, Hu Z, Liu J, Liu D, Lin B. Co-expression of Lewis y antigen with human epididymis protein 4 in ovarian epithelial carcinoma. PloS one. 2013;8(7):e68994.

38. Zhuang H, Hu Z, Tan M, Zhu L, Liu J, Liu D, Yan L, Lin B. Overexpression of Lewis y antigen promotes human epididymis protein 4-mediated invasion and metastasis of ovarian cancer cells. Biochimie. 2014;105:91–8.
39. Liu JJ, Lin B, Hao YY, Li FF, Liu DW, Qi Y, Zhu LC, Zhang SL, Iwamori M. Lewis(y) antigen stimulates the growth of ovarian cancer cells via regulation of the epidermal growth factor receptor pathway. Oncol Rep. 2010;23(3):833–41.
40. James NE, Chichester C, Ribeiro JR. Beyond the Biomarker: Understanding the Diverse Roles of Human Epididymis Protein 4 in the Pathogenesis of Epithelial Ovarian Cancer. Front Oncol. 2018;8:124.
41. Moore RG, Hill EK, Horan T, Yano N, Kim K, MacLaughlan S, Lambert-Messerlian G, Tseng YD, Padbury JF, Miller MC, et al. HE4 (WFDC2) gene overexpression promotes ovarian tumor growth. Scientific reports. 2014;4:3574.
42. Zhu L, Gao J, Hu Z, Schwab C, Zhuang H, Tan M, Yan L, Liu J, Zhang D, Lin B. Membranous expressions of Lewis y and CAM-DR-related markers are independent factors of chemotherapy resistance and poor prognosis in epithelial ovarian cancer. Am J Cancer Res. 2015;5(2):830–43.
43. Ribeiro JR, Schorl C, Yano N, Romano N, Kim KK, Singh RK, Moore RG. HE4 promotes collateral resistance to cisplatin and paclitaxel in ovarian cancer cells. J Ovarian Res. 2016;9(1):28.
44. James NE, Cantillo E, Oliver MT, Rowswell-Turner RB, Ribeiro JR, Kim KK, Chichester CO 3rd, DiSilvestro PA, Moore RG, Singh RK, et al. HE4 suppresses the expression of osteopontin in mononuclear cells and compromises their cytotoxicity against ovarian cancer cells. Clin Exp Immunol. 2018;193(3):327–40.
45. James NE, Oliver MT, Ribeiro JR, Cantillo E, Rowswell-Turner RB, Kim KK, Chichester CO 3rd, DiSilvestro PA, Moore RG, Singh RK, et al. Human Epididymis Secretory Protein 4 (HE4) Compromises Cytotoxic Mononuclear Cells via Inducing Dual Specificity Phosphatase 6. Front Pharmacol. 2019;10:216.
46. Lou T, Zhuang H, Liu C, Zhang Z. HDAC3 positively regulates HE4 expression to promote ovarian carcinoma progression. Arch Biochem Biophys. 2019;675:108044.
47. Wang J, Deng L, Zhuang H, Liu J, Liu D, Li X, Jin S, Zhu L, Wang H, Lin B. Interaction of HE4 and ANXA2 exists in various malignant cells-HE4-ANXA2-MMP2 protein complex promotes cell migration. Cancer Cell Int. 2019;19:161.
48. Sato S, Itamochi H. Dual specificity phosphatase 6 as a new therapeutic target candidate for epithelial ovarian cancer. Ann Transl Med. 2019;7(Suppl 8):373.

Figures

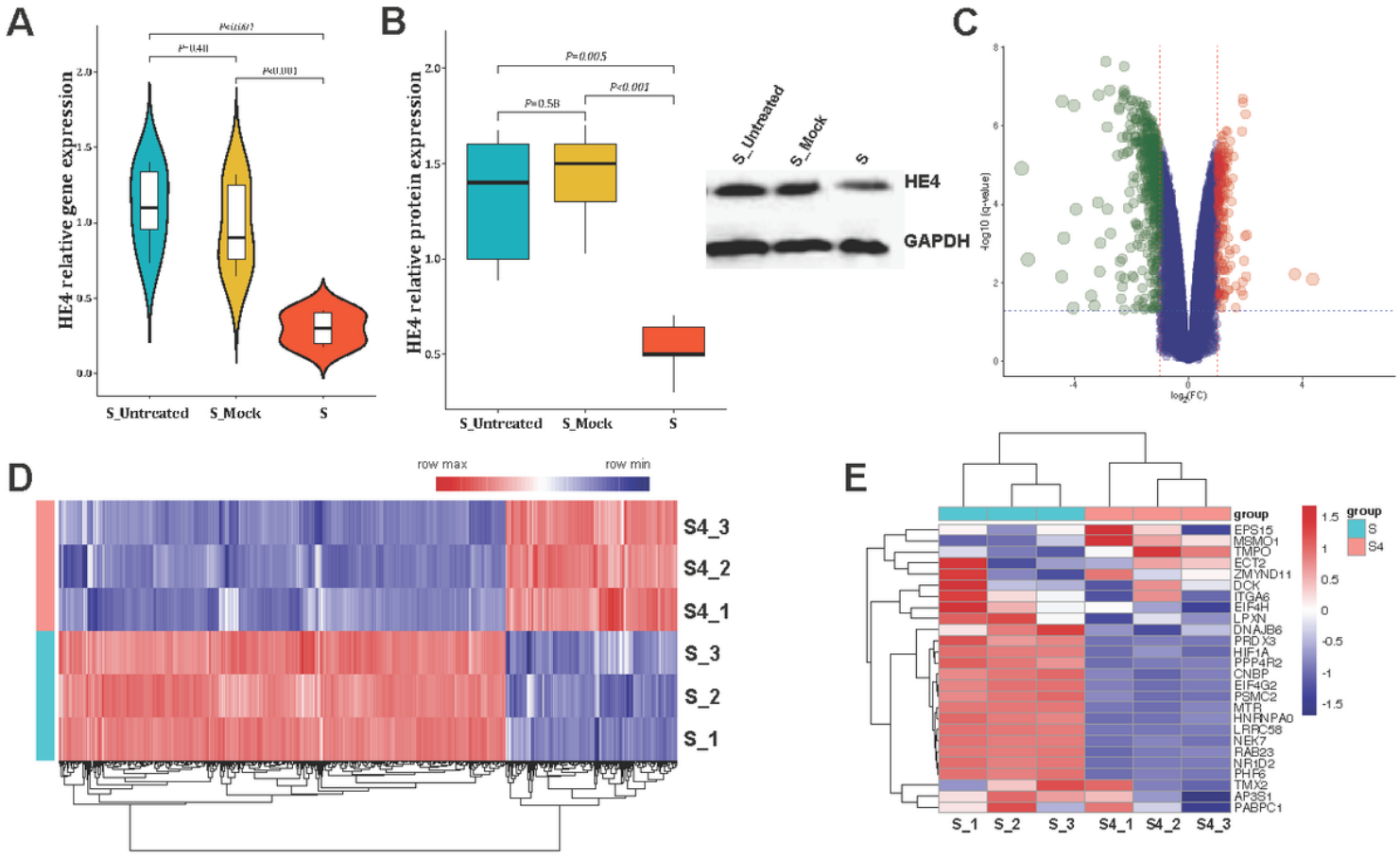

Figure 1

Confirmation of transfection in ovarian cancer cell line ES-2 and the identification of differentially expressed genes (DEGs) in response to active HE4 stimulation in ES-2 cells A. Quantitative real-time PCR results showing the gene expression of HE4 after HE4 shRNA transfection in ovarian cancer cell line ES-2. B. Western blotting results showing the protein expression of HE4 after HE4 shRNA transfection. A part of the plot is from our previously published paper [5]. C. Volcano plot of the 18,398 expressed genes. The red and green colors represent genes up- and downregulated in response to HE4 activation in ES-2 cells. Gene symbols of DEGs showing log2|fold-change|≥ 3 are listed in the plot. D. Clustering heatmap of the 713 genes exhibiting significantly differential expression; significant DEGs were defined based on log2|fold-change| values ≥ 1 and p-values < 0.05. E. Heatmap showing representative DEGs in ovarian cancer cells. The color key from blue to red indicates low to high gene expression, respectively.

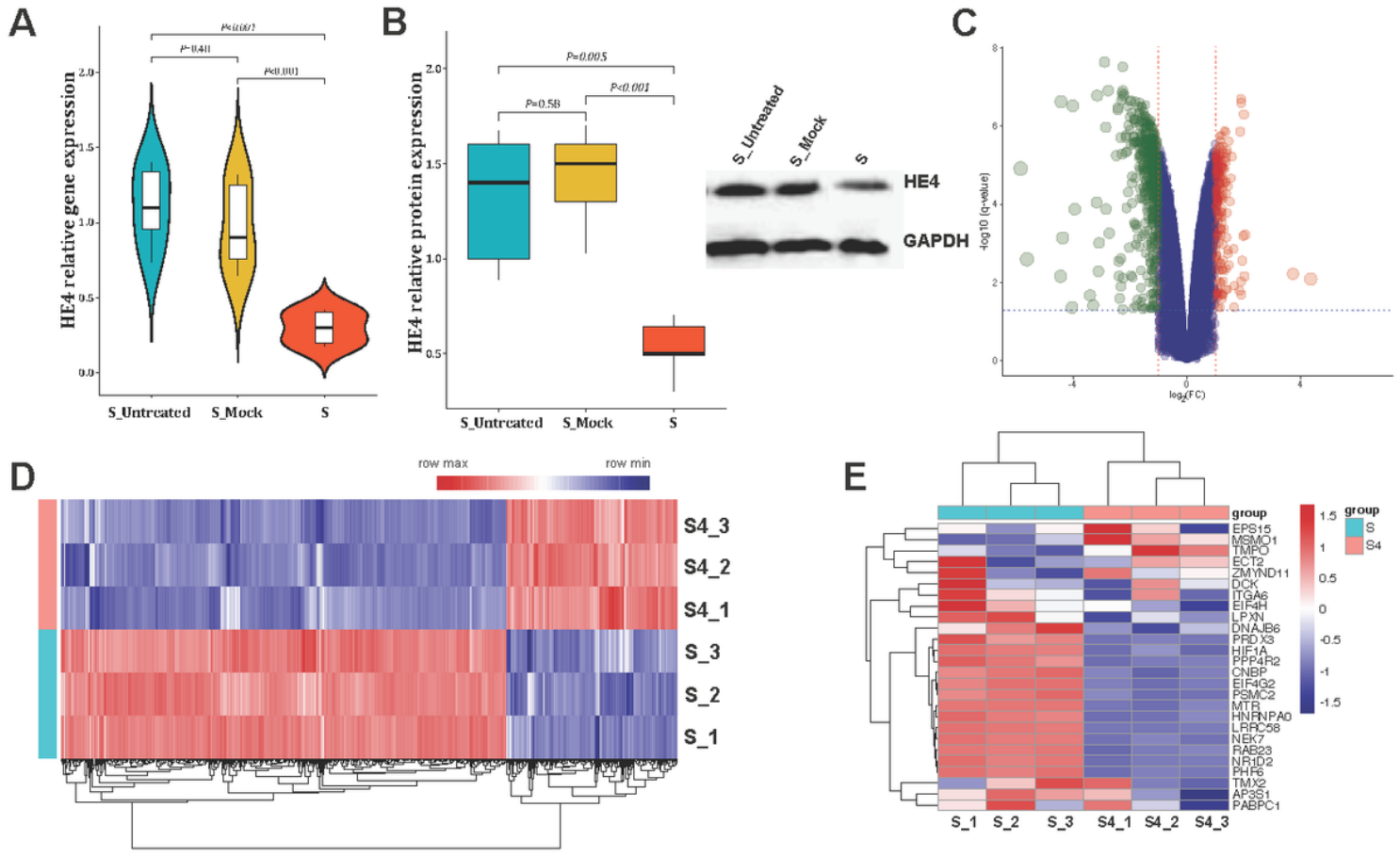

Figure 1

Confirmation of transfection in ovarian cancer cell line ES-2 and the identification of differentially expressed genes (DEGs) in response to active HE4 stimulation in ES-2 cells A. Quantitative real-time PCR results showing the gene expression of HE4 after HE4 shRNA transfection in ovarian cancer cell line ES-2. B. Western blotting results showing the protein expression of HE4 after HE4 shRNA transfection. A part of the plot is from our previously published paper [5]. C. Volcano plot of the 18,398 expressed genes. The red and green colors represent genes up- and downregulated in response to HE4 activation in ES-2 cells. Gene symbols of DEGs showing log2|fold-change|≥ 3 are listed in the plot. D. Clustering heatmap of the 713 genes exhibiting significantly differential expression; significant DEGs were defined based on log2|fold-change| values ≥ 1 and p-values < 0.05. E. Heatmap showing representative DEGs in ovarian cancer cells. The color key from blue to red indicates low to high gene expression, respectively.

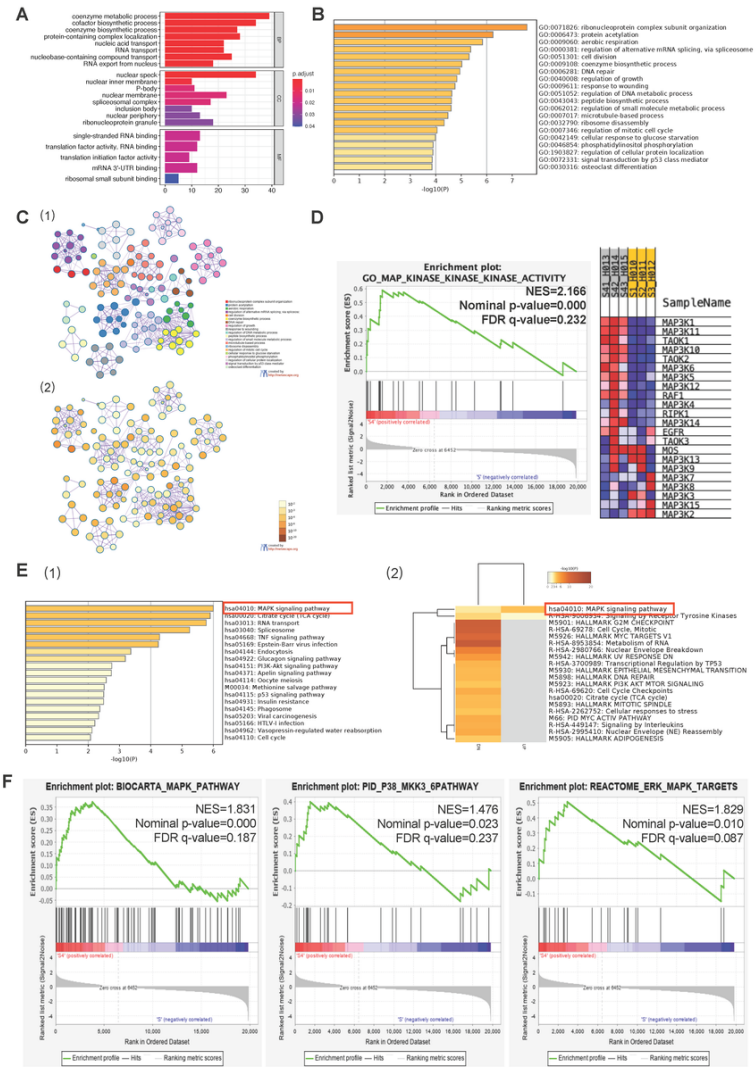

Figure 2

Gene ontology (GO) and pathway enrichment of 713 DEGs A. GO enrichment analysis of 713 DEGs in “clusterProfiler” package of R, sorted in ascending order of the adjusted p value of the GO list. BP, biological process; CC, cellular component; MF, molecular function. B. Heatmap showing GO enrichment of all DEGs generated by Metascape and sorted based on the value of −Log10(P-value). The GO ID items are shown in the right panel. C. (1) Network layout of the clusters generated with the complete DEGs regulated by HE4 in ovarian cancer cells, where each node represents an enriched term and is colored by its cluster ID. Its size is proportional to the number of input genes falling into that term. One term from each cluster was selected and its term description is shown as a label. (2) Network of enriched terms colored based on the P-value, where terms containing more genes tend to have a more significant P-value. D. GSEA shows that the ‘GO_MAP_KINASE_KINASE_KINASE_ACTIVITY’ gene-set, comprising genes specifically upregulated in S4 cells was enriched, compared to the case in S cells. A heatmap of genes related to the analyzed GeneSet is shown in the right panel. E. (1) KEGG Pathways enriched for all DEGs generated by Metascape and sorted based on values of −Log10(P-value). (2) Pathway enrichment analysis (gene sets including: KEGG, Hallmark Gene Sets, Reactome Gene Sets, Canonical, and BioCarta Gene Sets) of up- and downregulated gene lists generated by Metascape and sorted based on the value of −Log10(P-value). The pathway ID items are shown in the right panel. F. GSEA showed that the “BIOCARTA_MAPK_PATHWAY”, “PID_P38_MKK3_6ATHWAY”, and “REACTOME_ERK_MAPK_TARGETS” gene-sets comprising genes specifically upregulated in S4 cells were enriched, compared to the case in S cells.

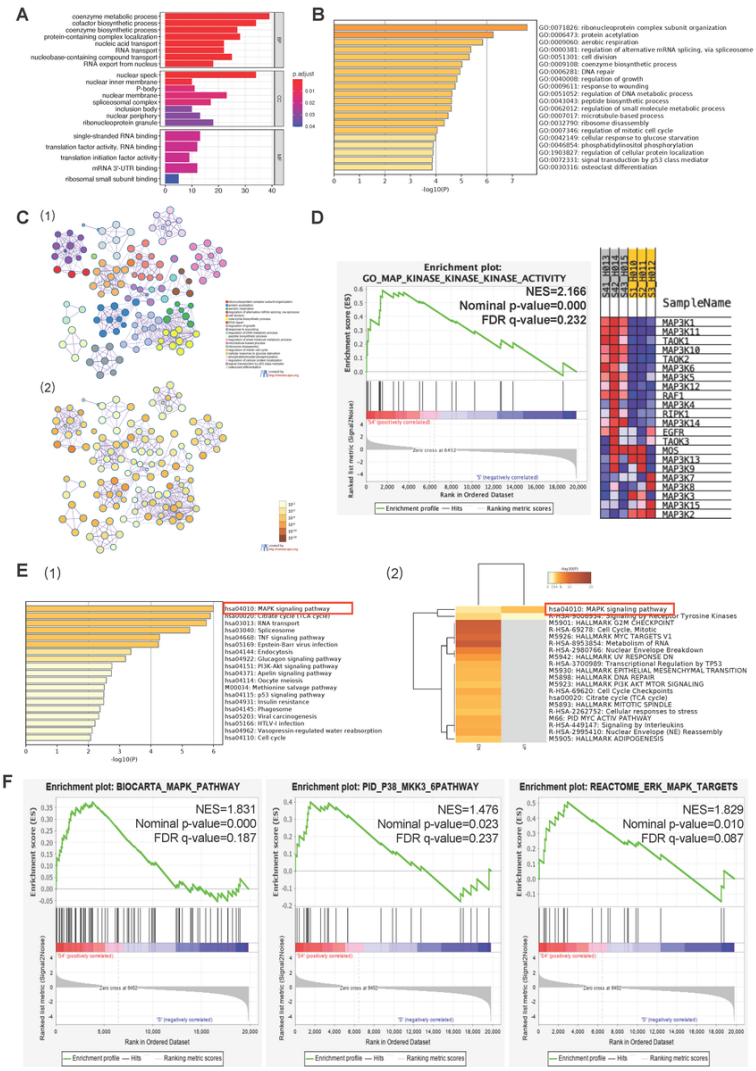

Figure 2

Gene ontology (GO) and pathway enrichment of 713 DEGs A. GO enrichment analysis of 713 DEGs in “clusterProfiler” package of R, sorted in ascending order of the adjusted p value of the GO list. BP, biological process; CC, cellular component; MF, molecular function. B. Heatmap showing GO enrichment of all DEGs generated by Metascape and sorted based on the value of −Log10(P-value). The GO ID items are shown in the right panel. C. (1) Network layout of the clusters generated with the complete DEGs regulated by HE4 in ovarian cancer cells, where each node represents an enriched term and is colored by its cluster ID. Its size is proportional to the number of input genes falling into that term. One term from each cluster was selected and its term description is shown as a label. (2) Network of enriched terms colored based on the P-value, where terms containing more genes tend to have a more significant P-value. D. GSEA shows that the ‘GO_MAP_KINASE_KINASE_KINASE_ACTIVITY’ gene-set, comprising genes specifically upregulated in S4 cells was enriched, compared to the case in S cells. A heatmap of genes related to the analyzed GeneSet is shown in the right panel. E. (1) KEGG Pathways enriched for all DEGs generated by Metascape and sorted based on values of −Log10(P-value). (2) Pathway enrichment analysis (gene sets including: KEGG, Hallmark Gene Sets, Reactome Gene Sets, Canonical, and BioCarta Gene Sets) of up- and downregulated gene lists generated by Metascape and sorted based on the value of −Log10(P-value). The pathway ID items are shown in the right panel. F. GSEA showed that the “BIOCARTA_MAPK_PATHWAY”, “PID_P38_MKK3_6ATHWAY”, and “REACTOME_ERK_MAPK_TARGETS” gene-sets comprising genes specifically upregulated in S4 cells were enriched, compared to the case in S cells.

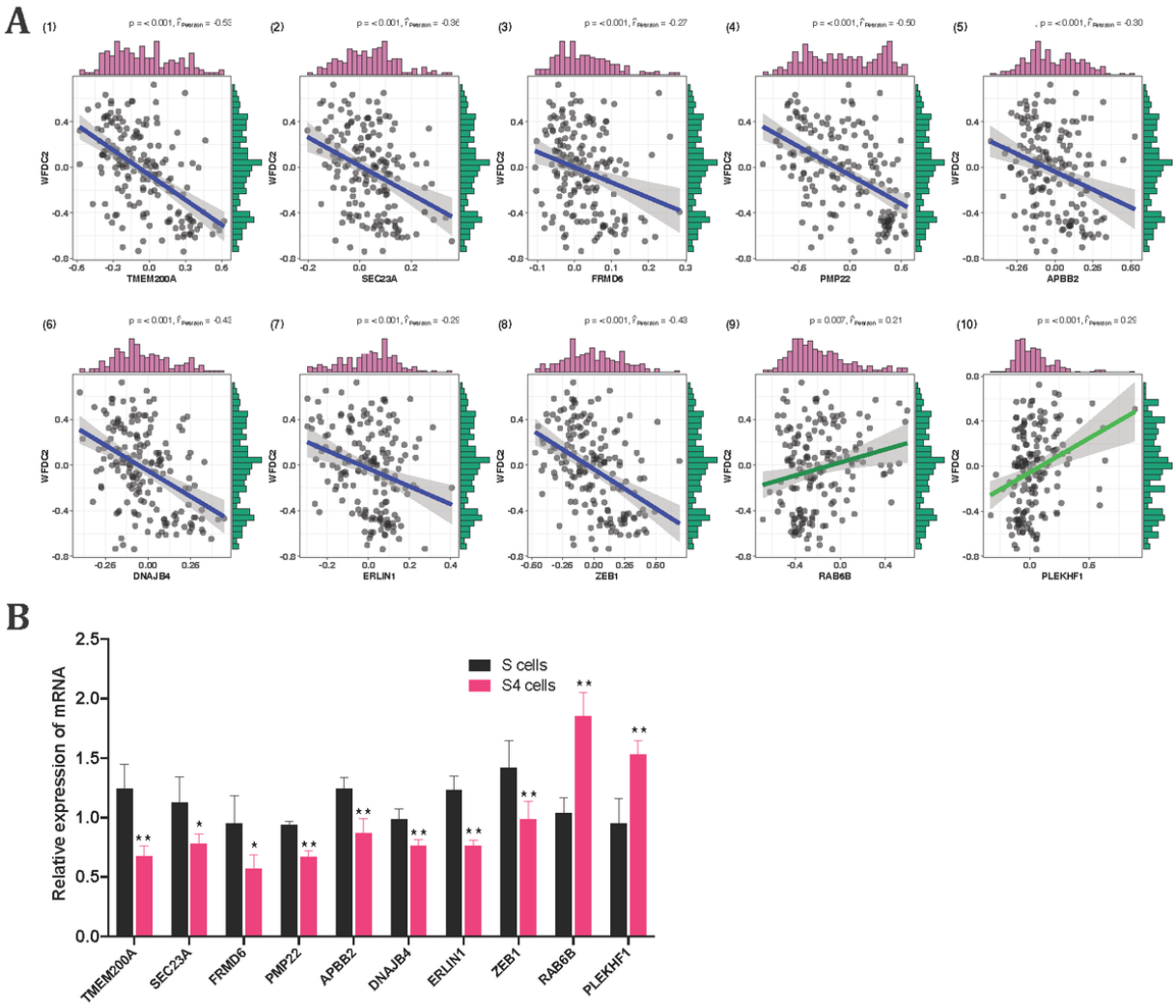

Figure 3

Correlation analysis of WFDC2-co-expressed genes and mRNA validation A. Pearson's correlation analysis using GSE51088 data. (1)–(8) are genes negatively correlated with WFDC2 (TMEM220A, SEC23A, FRMD6, PMP22, APBB2, DNAJB4, ERLIN1, and ZEB1) and (9) and (10) are genes positively correlated with WFDC2 (RAB6B, and PLEKHF1). B. Quantitative real-time PCR revealed the mRNA expression levels of 10 target genes in ovarian cancer cells (S4 vs. S). *P < 0.05, **P < 0.01.

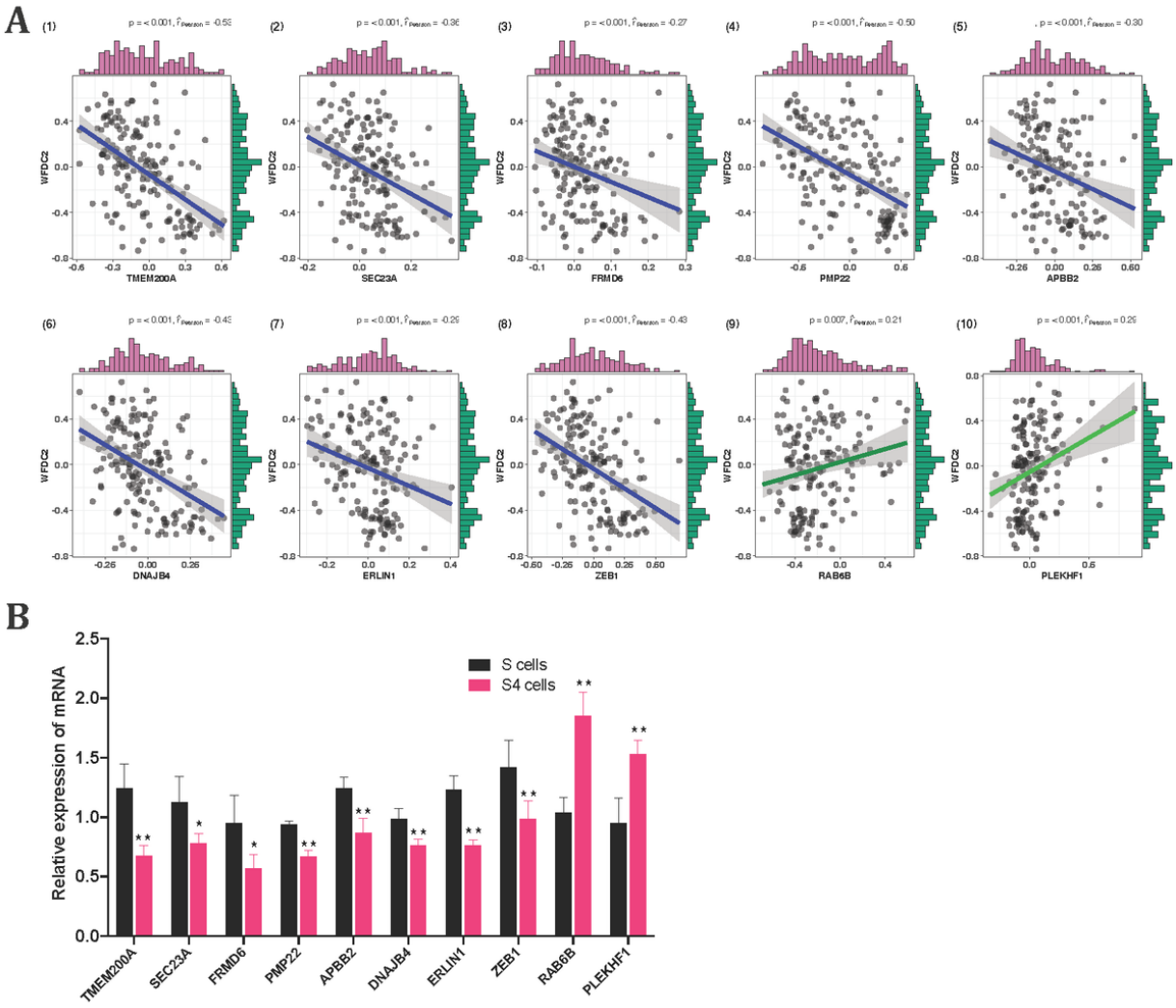

Figure 3

Correlation analysis of WFDC2-co-expressed genes and mRNA validation A. Pearson's correlation analysis using GSE51088 data. (1)–(8) are genes negatively correlated with WFDC2 (TMEM220A, SEC23A, FRMD6, PMP22, APBB2, DNAJB4, ERLIN1, and ZEB1) and (9) and (10) are genes positively correlated with WFDC2 (RAB6B, and PLEKHF1). B. Quantitative real-time PCR revealed the mRNA expression levels of 10 target genes in ovarian cancer cells (S4 vs. S). *P < 0.05, **P < 0.01.

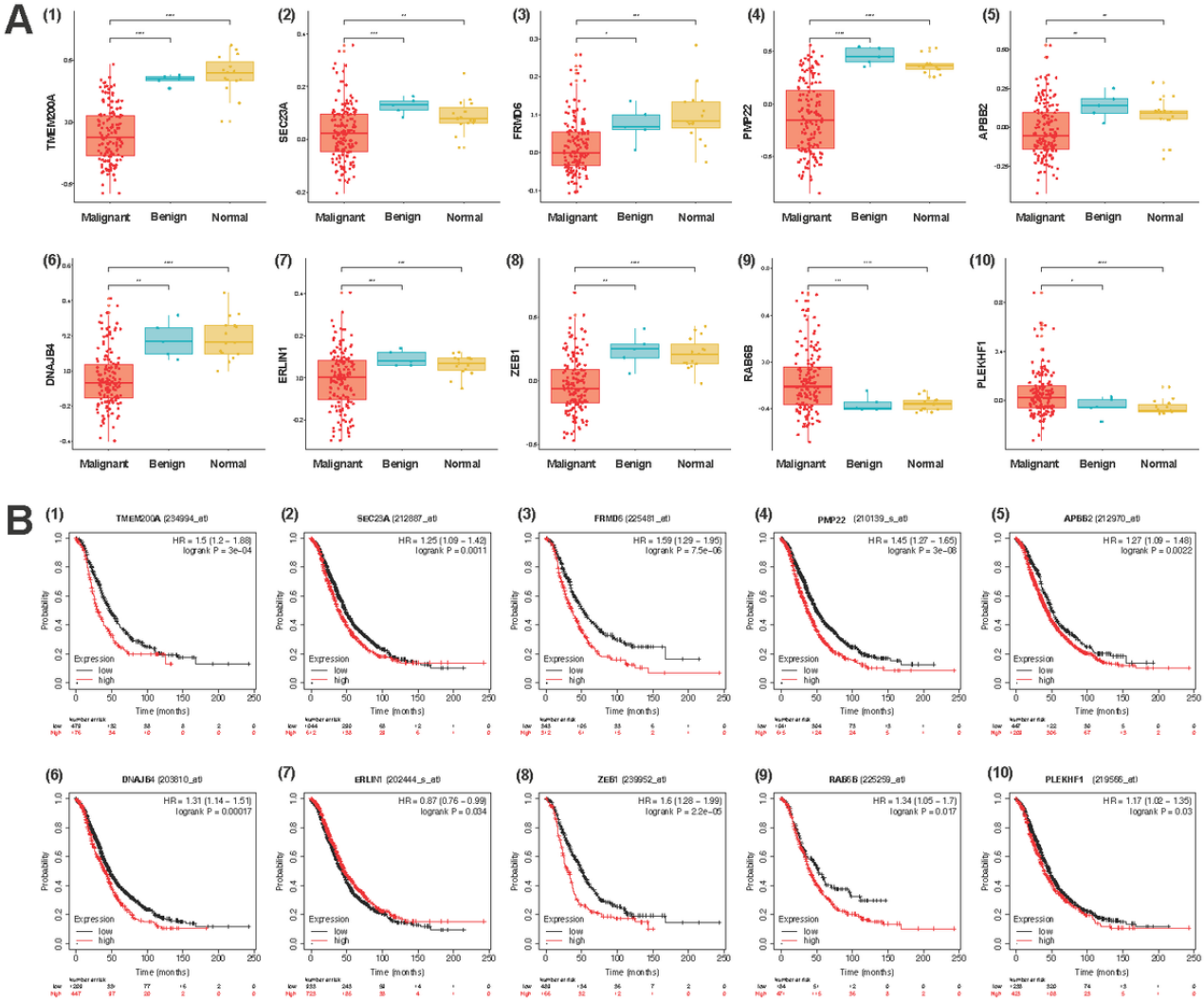

Figure 4

Clinical significance of 10 target genes A. Comparison of 10 target genes with tumor types by using GSE51088, which contains 152 samples of epithelial ovarian cancer (including 11 epithelial ovarian borderline tumors), 5 samples of normal ovarian tumors, and 15 samples of normal healthy ovarian tissues. (1)–(8) show genes (TMEM220A, SEC23A, FRMD6, PMP22, APBB2, DNAJB4, ERLIN1, and ZEB1) significantly downregulated in ovarian cancers, compared to those in ovarian benign tumors and normal tissues, and (9) and (10) show genes (RAB6B and PLEKHF1) that were markedly upregulated in ovarian cancers, compared to those in ovarian benign tumors and normal tissues. C. Kaplan–Meier survival analysis revealed that all ten correlated genes were strongly correlated with overall survival.

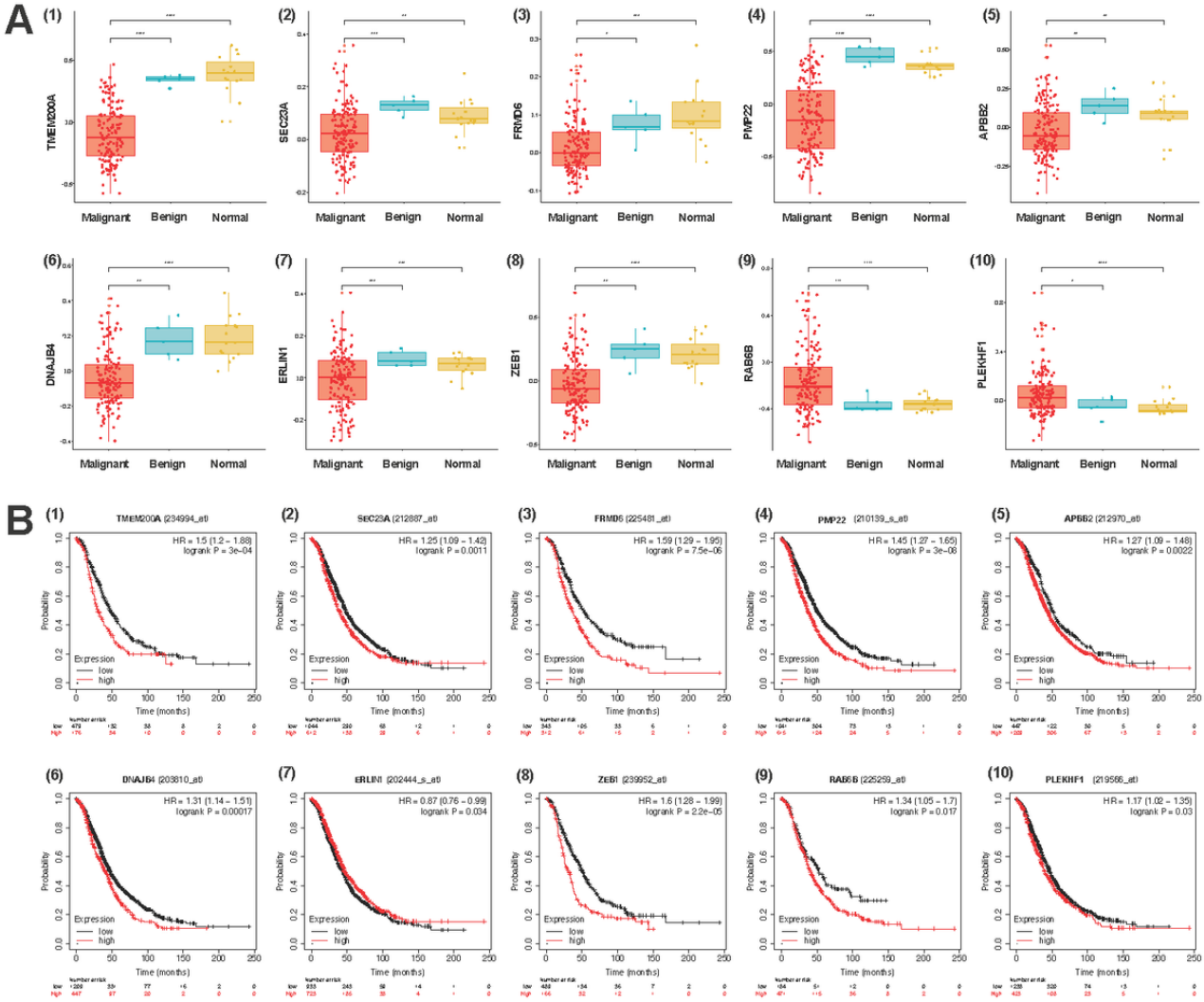

Figure 4

Clinical significance of 10 target genes A. Comparison of 10 target genes with tumor types by using GSE51088, which contains 152 samples of epithelial ovarian cancer (including 11 epithelial ovarian borderline tumors), 5 samples of normal ovarian tumors, and 15 samples of normal healthy ovarian tissues. (1)–(8) show genes (TMEM220A, SEC23A, FRMD6, PMP22, APBB2, DNAJB4, ERLIN1, and ZEB1) significantly downregulated in ovarian cancers, compared to those in ovarian benign tumors and normal tissues, and (9) and (10) show genes (RAB6B and PLEKHF1) that were markedly upregulated in ovarian cancers, compared to those in ovarian benign tumors and normal tissues. C. Kaplan–Meier survival analysis revealed that all ten correlated genes were strongly correlated with overall survival.

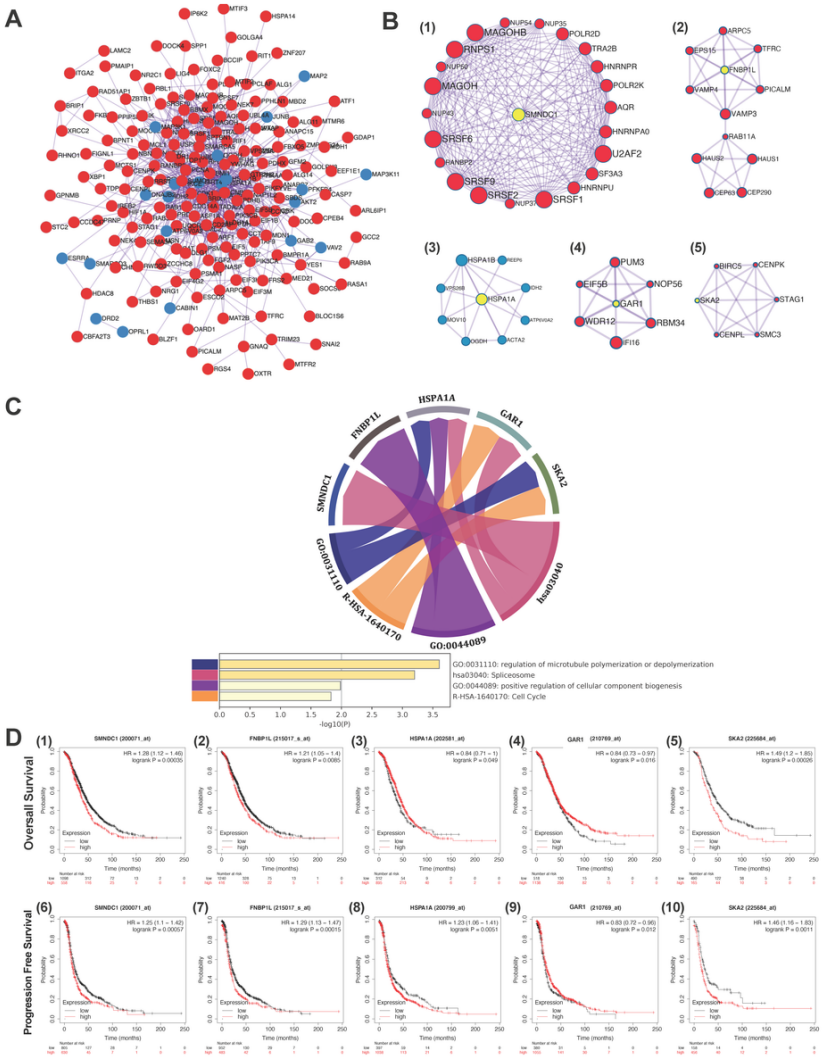

Figure 5

Protein-protein interaction (PPI) network construction, identification of MCODE modules, and clinical significance of module seeds A. PPI networks of all DEGs was constructed using Metascape. Red and blue represent down-and up-regulated genes, respectively. B. Five MCODEs identified in the PPI network with MCODE scores > 2. The yellow color represents the seed nodes of each MCODE module; the label size was determined according to the degree of connectivity. The red and blue colors represent the down- and upregulated genes, respectively. C. GO and KEGG pathway enrichment analysis of seeds of the 5 MCODE modules generated by Metascape. D. Kaplan–Meier survival analysis revealed that all five seed genes were significantly correlated with prognosis, both with regard to overall survival ((1)–(5)) and progression free survival ((6)–(10)).

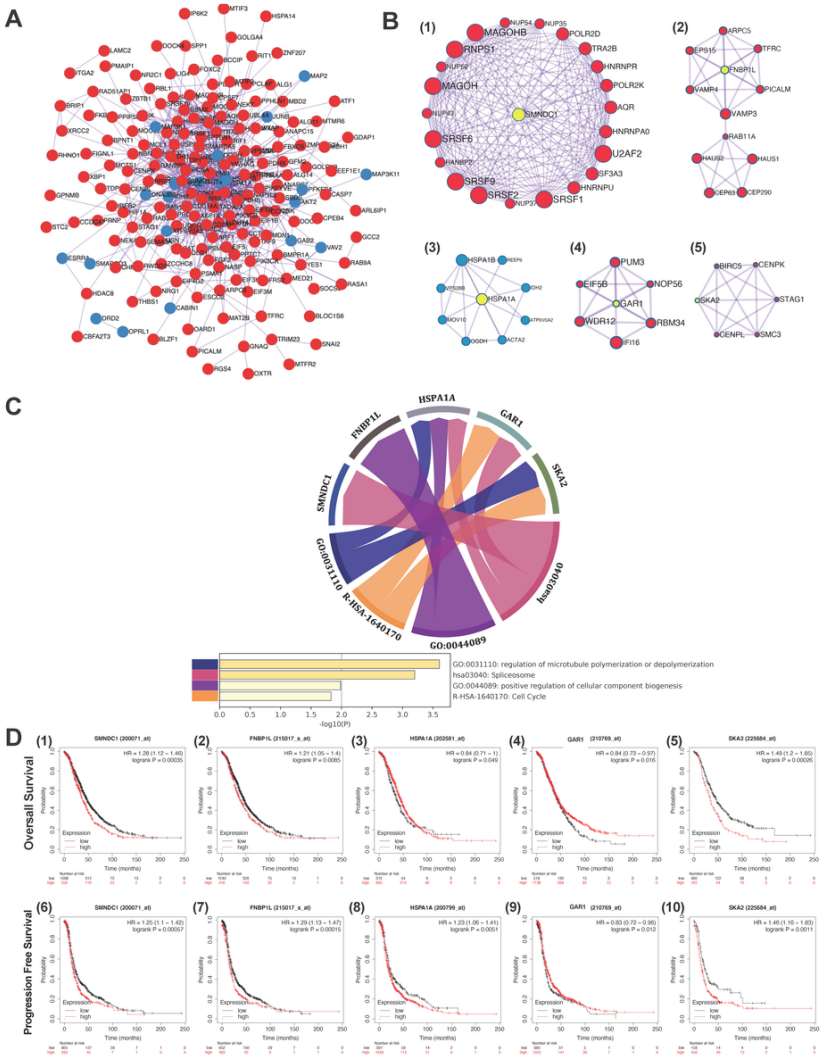

Figure 5

Protein-protein interaction (PPI) network construction, identification of MCODE modules, and clinical significance of module seeds A. PPI networks of all DEGs was constructed using Metascape. Red and blue represent down-and up-regulated genes, respectively. B. Five MCODEs identified in the PPI network with MCODE scores > 2. The yellow color represents the seed nodes of each MCODE module; the label size was determined according to the degree of connectivity. The red and blue colors represent the down- and upregulated genes, respectively. C. GO and KEGG pathway enrichment analysis of seeds of the 5 MCODE modules generated by Metascape. D. Kaplan–Meier survival analysis revealed that all five seed genes were significantly correlated with prognosis, both with regard to overall survival ((1)–(5)) and progression free survival ((6)–(10)).

Supplementary Files

This is a list of supplementary files associated with this preprint. Click to download.

- SupplementaryTable1.xlsx
- SupplementaryTable1.xlsx
- SupplementaryTable2.xlsx
- SupplementaryTable2.xlsx
- SupplementaryTable3.xlsx
- SupplementaryTable3.xlsx
- SupplementaryTable4.xlsx
- SupplementaryTable4.xlsx
- SupplementaryTable5.xlsx
- SupplementaryTable5.xlsx